JGR Oceans

RESEARCH ARTICLE
10.1029/2019JC015287

Key Points:
- Fluxes of biogenic particles were much higher during La Niña years in the deep Eastern Tropical Pacific
- Biogenic carbon export was estimated based on the observed particle fluxes and empirical equations for the vertical attenuation of carbon flux
- CO_2 outgassing was considerably suppressed by an enhanced biological pump during La Niña years

Correspondence to:
J. Hwang,
jeomshik@snu.ac.kr

Citation:
Kim, H. J., Kim, T.-W., Hyeong, K., Yeh, S.-W., Park, J.-Y., Yoo, C. M., & Hwang, J. (2019). Suppressed CO_2 Outgassing by an Enhanced Biological Pump in the Eastern Tropical Pacific. *Journal of Geophysical Research: Oceans*, *124*, 7962–7973. https://doi.org/10.1029/2019JC015287

Received 15 MAY 2019
Accepted 28 SEP 2019
Accepted article online 25 OCT 2019
Published online 19 NOV 2019

Manuscript revised for *Journal of Geophysical Research: Oceans*

Suppressed CO_2 Outgassing by an Enhanced Biological Pump in the Eastern Tropical Pacific

Hyung Jeek Kim[1], Tae-Wook Kim[2], Kiseong Hyeong[1], Sang-Wook Yeh[3], Jong-Yeon Park[4], Chan Min Yoo[1], and Jeomshik Hwang[5]

[1]Deep-sea and Seabed Mineral Resources Research Center, Korea Institute of Ocean Science & Technology, Busan, South Korea, [2]Division of Environmental Science and Ecological Engineering, Korea University, Seoul, South Korea, [3]Department of Environmental Marine Science, Hanyang University, Ansan, South Korea, [4]Department of Earth and Environmental Sciences, Chonbuk National University, Jeonju, South Korea, [5]School of Earth and Environmental Sciences/Research Institute of Oceanography, Seoul National University, Seoul, South Korea

Abstract The Eastern Tropical Pacific (ETP) is the largest oceanic source of carbon dioxide (CO_2) to the atmosphere. Sinking particle fluxes at a depth of 4,950 m (50 m above the seafloor) in the ETP were monitored from 2003 to 2013, during which the Pacific decadal oscillation (PDO) shifted from a positive to negative phase. We show a disproportionate increase in the efficiency of the biological pump in this region relative to the increase in primary production that occurred during La Niña years following the shift of the PDO in 2008. Biogenic carbon export from the surface mixed layer was estimated from the observed particulate organic carbon and inorganic carbon fluxes at a depth of 4,950 m and from empirical equations of the vertical attenuation of carbon flux. Enhanced biological carbon export accounted for 2.3–5.5 mol C m^{-2} $year^{-1}$ during the La Niña events. Despite a large uncertainty associated with these estimates, we propose that CO_2 outgassing was largely suppressed by an enhanced biological pump during the La Niña events in the negative PDO phase.

Plain Language Summary We examined the composition and flux of particles sinking to the deep Eastern Tropical Pacific from 2003 to 2013. This region is known as the largest oceanic source of CO_2 to the atmosphere. We observed that the flux of particulate organic and inorganic carbon to a depth of 4,950 m increased as the climate variability called the "Pacific decadal oscillation" shifted from a positive to negative phase (i.e., more La Niña events) in 2008. The biological pump efficiency (i.e., how efficiently biological production of organic matter is transported to the deep ocean) also increased during La Niña years. To investigate how biological production affects the CO_2 exchange with the atmosphere, we estimated the export of carbon from the surface layer based on our flux data at 4,950 m and the current understanding of carbon flux attenuation with depth. CO_2 outgassing was largely suppressed by an enhanced biological pump during the La Niña events in the negative PDO phase.

1. Introduction

Upwelling in the Eastern Tropical Pacific (ETP) reportedly contributes up to 50% of new biological production in the global oceans (Barber & Chavez, 1991; Loubere, 2000) and thus plays a critical role in Earth's carbon cycle. This region is also known to be the largest oceanic source of CO_2 to the atmosphere due to the upwelling of CO_2-rich deep water (Feely et al., 2006; Takahashi et al., 2003, 2009). The Pacific decadal oscillation (PDO) is the dominant source of sea surface temperature (SST) variability in the Pacific on low-frequency, decadal timescales (Newman et al., 2003), and influences the physical and biological conditions of the ETP (Folland et al., 2002; Peterson & Schwing, 2003). SST in the ETP is higher/lower during positive/negative PDO (Figure 1). Therefore, it is important to understand how biological processes and CO_2 outgassing in the ETP are influenced by the PDO. The biological response to natural climate variability in the ETP is poorly understood because of the paucity of long-term observations. In particular, the role of enhanced upwelling in CO_2 cycling in this region has not been addressed.

The ETP underwent a switch from a positive PDO to a negative phase in the late 2000s (Litzow & Mueter, 2014; Figures 1 and 2a). Frequent La Niña events have occurred since 2008 and have strengthened the impact of the negative PDO (Tollefson, 2014; Wang et al., 2014). Enhanced upwelling during a La Niña period may stimulate two processes in this region with opposing consequences for CO_2 flux between the ocean

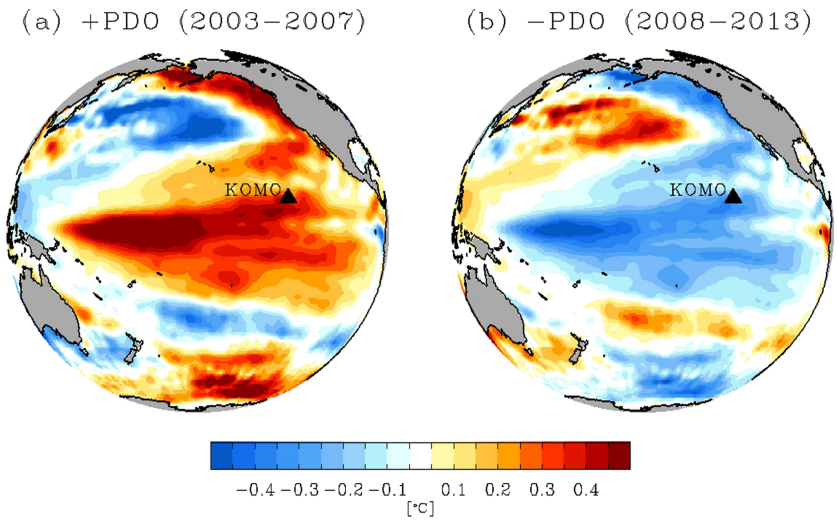

Figure 1. Sea surface temperature (SST) anomalies observed during (a) 2003–2007 in a positive PDO and (b) 2008–2013 in a negative PDO. The anomalies are defined as deviations from the monthly means over the period 2003–2012 and were averaged over December–May. The SST data were obtained from the NOAA optimum interpolation SST product that combines observations from satellites, ships, and buoys (https://www.esrl.noaa.gov; Reynolds et al., 2007). The triangle represents Station KOMO, where particle samples were collected monthly from 2003 to 2013.

and atmosphere. Upwelling of CO_2-rich deep water will facilitate the efflux of CO_2 to the atmosphere. In contrast, the biological pump, which facilitates sequestration of atmospheric CO_2 into the deep ocean via primary production, can be boosted by additional nutrient supply. The biological pump is a critical system in the ETP and needs to be evaluated quantitatively to improve our understanding of its role in modulating the atmospheric CO_2 level. By measuring the export of particulate organic carbon (POC) using time-series sediment traps and determining concurrent net primary production (NPP), one can better evaluate the functioning of the biological pump. In the mid-1990s, primary production and carbon flux responses to the ENSO (El Niño Southern Oscillation) were studied in the ETP as a part of the United States Joint Global Ocean Flux Study (Bacon et al., 1996; Buesseler et al., 1995; Murray et al., 1996). These studies found that the ratio of POC export to primary production (*e*-ratio) varied from 0.03 to 0.23, with potentially higher values during a cold period (non-El Niño) than during the preceding El Niño event. Attenuation in POC flux with increasing depth has been extensively studied in the ETP (Berelson, 2001; Buesseler & Boyd, 2009) and has been simulated using an equation known as the "Martin curve" (Berelson, 2001; Martin et al., 1987). Therefore, the POC export may be estimated from POC flux measurements at depth. Because continuous data for export and production over an extended time period are difficult to obtain, time-series POC flux measurements at depth may provide an alternative way to estimate the POC export.

We obtained time-series data for the biogenic particle composition and particle flux at a depth of 4,950 m in the ETP from July 2003 to July 2013. This study period spanned a regime shift in the PDO in 2008 from a positive to a negative phase (Figure 2a) and provided us with an opportunity to examine the biological response. We investigated how the role of biological pump changed as the PDO phase shifted, based on our particle flux data and the knowledge of particle flux attenuation from previous studies (Berelson, 2001; Buesseler & Boyd, 2009; Martin et al., 1987).

2. Methods

The Korea Institute of Ocean Science and Technology has maintained a long-term monitoring station in the ETP (Station KOMO; 10.5°N and 131.2°W; Figure 1) since 2003 to investigate the biogeochemical cycling of organic carbon (Kim et al., 2011). SST, sea surface salinity (SSS), and wind speed at this site are largely influenced by seasonal and interannual migration of the intertropical convergence zone and ENSO events (Amador et al., 2006; Kim et al., 2011).

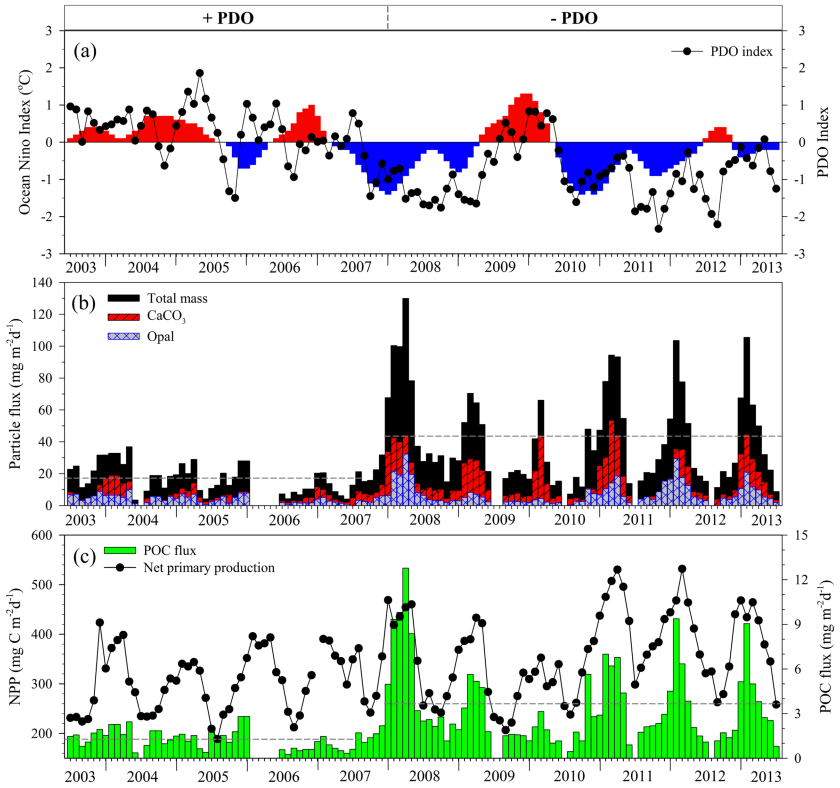

Figure 2. (a) SST anomalies observed in the Nino 3.4 region (red and blue bars denote the positive and negative anomalies, respectively). The Pacific decadal oscillation (PDO) shifted from a positive to negative phase in 2008 (Wu, 2013). (b) Fluxes of total mass, $CaCO_3$, and biogenic opal at Station KOMO from July 2003 to June 2013. (c) Satellite-derived net primary production (NPP) and observed particulate organic carbon (POC) flux. Horizontal dashed lines in (b) and (c) indicate average values of total particle flux and POC flux from July 2003 to June 2007 and the negative PDO–La Niña period (from July 2007 to June 2009 and July 2010 to June 2013). Blank areas indicate no data.

Sinking particles were collected monthly by a sediment trap (PARFLUX Mark 78H-21; McLane Laboratory) moored at 4,950 m depth (50 m above the seafloor). Samples were collected monthly from July 2003 to July 2013 (supporting information, Data Set S1). The trap mooring array was recovered and redeployed once a year. Sinking particles were also collected intermittently at depths of 1,200 and 4,500 m (Data Set S1). Each sampling cup was filled with filtered seawater collected from the deployment depth and treated with sodium borate-buffered 10% formalin solution. Recovered samples were stored in a refrigerator at 2–4 °C. Sample analyses were performed within a few months of sampling.

Zooplankton specimens larger than 1 mm were removed using tweezers upon inspection with the naked eye. Each trap sample was split into five equal aliquots using a McLane wet sample divider (WSD-10). Three aliquots were rinsed with ultrapure (Milli-Q) water, freeze-dried, and weighed for gravimetric determination of total particle flux. Total particulate carbon content was determined using an elemental analyzer (Carlo-Erba 1110 CNS) with a precision of <1.2% relative standard deviation (RSD). Particulate inorganic carbon (PIC) content was analyzed using a total inorganic carbon analyzer (UIC CO_2 coulometer; model CM5014) with <1% RSD. Calcium carbonate ($CaCO_3$) content was calculated by multiplying the PIC content by a conversion factor of 8.33 (the weight ratio of $CaCO_3$ to carbon; Wefer & Fischer, 1993). POC content was estimated as the difference between total carbon and inorganic carbon contents. A direct decarbonation method using sulfurous acid was also used for determination of POC contents of a set of samples ($n = 9$; <0.5% RSD; Kim et al., 2011; Verardo et al., 1990). Both methods agreed within 0.4%. Biogenic opal content was determined following a sequential alkaline leaching method with <3% RSD (DeMaster, 1981). Planktonic foraminifera flux was determined by picking individual foraminifera tests under the microscope (Zeiss Stemi SV 11; 10×) and weighing. The presence of coccoliths was verified by examination under the microscope. Coccolithophore flux was estimated as the difference between the $CaCO_3$ and foraminifera fluxes.

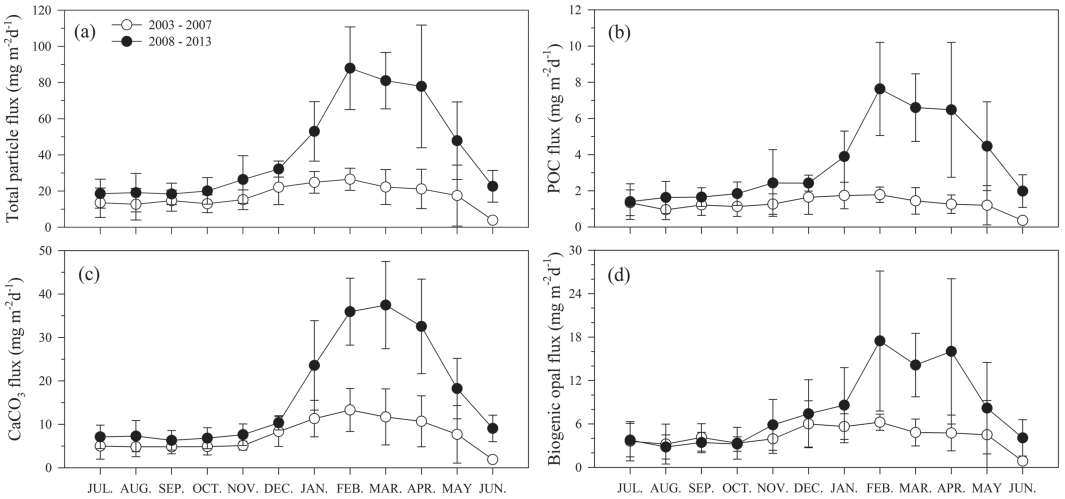

Figure 3. Monthly averaged fluxes of (a) total particle mass, (b) particulate organic carbon POC, (c) calcium carbonate ($CaCO_3$), and (d) biogenic opal at Station KOMO. Data are presented separately for two periods: July 2003 to June 2007 (open circles) and July 2007 to June 2009, July 2010 to June 2013 (solid circles). Error bars are one standard deviation of the monthly data.

NPP was estimated from 9-km resolution monthly satellite chlorophyll data using the vertically generalized production model (Behrenfeld & Falkowski, 1997). The model is based on a temperature-dependent description of MODIS chlorophyll-specific photosynthetic efficiency, which utilizes day length, surface chlorophyll-a concentration, SST, and photosynthetically available radiation (www.science.oregonstate.edu/ocean.productivity). The median value of NPP in the 1° × 1° grid box surrounding our study site was taken to examine biological activity in the ETP and for comparison with the particle flux data. The monthly SST data were obtained from the NOAA optimum interpolation SST product that combines observations from satellites, ships, and buoys (http://www.esrl.noaa.gov; Reynolds et al., 2007), with a spatial resolution of 1° × 1°. The monthly SSS data were obtained from the Global Ocean Data Assimilation System, produced at the National Center for Environmental Prediction (Behringer & Xue, 2004). The data are estimated by assimilating ocean observations from Argo floats to a physical ocean model with a spatial resolution of 1° × 0.333° (longitude × latitude; Behringer & Xue, 2004).

3. Results

Details of the particle flux, composition, and their controlling factors for part of the observation period have been reported elsewhere (Kim et al., 2011, 2012). In this paper, we focus on the overall interannual variation of the particle flux and composition. Over the study period from July 2003 to July 2013, the total particle flux at 4,950 m varied from 3.5 to 130 mg·m^{-2}·day^{-1} with an average (±1 standard deviation) of 31.5 (±26) mg·m^{-2}·day^{-1} (Figure 2b). Total particle flux data exhibited a unimodal seasonal pattern: an average flux of 49.2 ± 31.0 mg·m^{-2}·day^{-1} for December–May and 18.8 ± 9.3 mg·m^{-2}·day^{-1} for June–November (Figure 2b). Fluxes of biogenic particles such as POC, opal, and $CaCO_3$ exhibited seasonal and interannual variations similar to that of the total particle flux (Figure 2). Average fluxes of $CaCO_3$, biogenic opal, and POC over the entire study period were 12.9 ± 11.6, 6.2 ± 5.7, and 2.5 ± 2.3 mg·m^{-2}·day^{-1}, respectively. The ratio of PIC flux to POC flux varied between 0.2 and 1.7, with an average of 0.65. The fluxes of planktonic foraminifera and coccolithophores accounted for ~39% and ~61% of the $CaCO_3$ flux, respectively (the coccolithophore flux is the difference between the $CaCO_3$ and foraminifera flux).

A notable feature of the interannual variations in total particle flux is a shift from a low-flux period (2003–2007) to a high-flux period (2008–2013). POC flux varied in proportion to the total particle flux and there was a clear shift in POC flux toward higher values after 2007 (Figure 2c). The increase in all biogenic particle fluxes from a positive to negative PDO phase was most conspicuous over December–May (Figure 3). The average POC flux for December–May increased from 1.5 to 4.7 mg·m^{-2}·day^{-1} between the two periods. The ratio of PIC flux to POC flux did not show any significant temporal trend between the two periods.

The contribution of $CaCO_3$ increased in the latter period, resulting in a slight decrease in the opal flux to $CaCO_3$ flux ratio from 0.54 to 0.45 and the opal flux to coccoliths flux ratio from 1.25 to 0.99.

4. Discussion

4.1. Sources of Sinking Particles

The POC flux has shown a marked increase since mid-2007. We first examined the possibility of an allochthonous source of POC to the mooring site. Seasonal pulses in POC flux agree well with the temporal variation in satellite-derived NPP, particularly in years of high POC flux. Although coupling between biological production in the surface ocean and particle flux at depth is clear at a seasonal scale, the timing of each annual peak in POC flux does not exactly match that in NPP (Figure 2c). This might reflect time lags of 20–30 days related to particle sinking (Berelson, 2001; Honjo et al., 1995).

We used satellite-NPP data over a 1° × 1° area around Station KOMO for comparison with the particle fluxes. Horizontal distribution of the NPP was homogeneous within 2−3° from Station KOMO, and hence our 1° × 1° data can represent the NPP at the mooring site. Subsurface lateral transport of particles was also considered. Based on the current speeds measured at a depth of 120 m (80 cm/s) at a Tropical Atmosphere Ocean array (Kessler, 2006; Kessler et al., 1995) and at a depth of 1,235 m (10 cm/s) at the mooring site, the maximum range of lateral transport of particles during vertical transit would be <100 km. Northward transport of particles from more productive equatorial regions is not likely because of the strong eastward North Equatorial Countercurrent between 5 and 10°N.

We also examined the potential influence of resuspended sediment on sinking particles. Biogenic material (i.e., the sum of $CaCO_3$, opal, and organic matter = POC × 1.88; the ratio of organic matter to POC was taken from Lam et al., 2011) accounted for 75 ± 8% of total particulate mass. The remaining fraction included aeolian lithogenic material flux and resuspended sediment. Current speed measured daily at 15 m above the seafloor (35 m below the sediment trap) varied from 0.3 to 14.5 cm/s (average = 3.6 cm/s) over the periods from July 2003 to June 2009 and August 2011 to September 2012. These values are not high enough to resuspend deep-sea sediment and affect the trapping efficiency (Baker et al., 1988; Honjo et al., 1995). Particle fluxes do not show any correlation with the measured current speed (not shown). Moreover, POC and $CaCO_3$ contents in the surface sediments (0–1 cm horizon) at and around Station KOMO were only 0.7% and 0.12%, respectively (Kim et al., 2015). Therefore, the influence of resuspended sediment on POC and PIC fluxes is likely to be minimal. Based on these considerations, we consider that POC and PIC fluxes were derived mainly from biological production in the surface water at or around the study site.

4.2. Relationship Between the Particle Flux and Climate Variability in the ETP

Primary production in the ETP is influenced by the upwelling of nutrient-rich deep water (Pennington et al., 2006; Strutton & Chavez, 2000). As of mid-2007, the PDO shifted to its negative phase with an increasing frequency of La Niña events (Figure 2a). The Ocean Niño Index (i.e., the SST departure from monthly climatological mean values in the Niño 3.4 region) also showed negative values after mid-2007. The period from December 2009 to May 2010 was an exception, during which there was a departure to more positive values of Ocean Niño Index. In this period, POC flux was significantly lower than in the other years of the negative PDO phase. Therefore, ENSO appears to influence the POC flux more directly than PDO, which has a much lower frequency. In addition, PDO has more visible climatic fingerprints in the North Pacific, whereas ENSO mainly affects the tropics (Mantua & Hare, 2002; Newman et al., 2016). It is unclear whether the La Niña effects on the POC flux were enhanced by the negative phase of PDO. Ideally, much longer time-series data, including various combinations of positive and negative PDO phases and El Niño and La Niña, are needed to understand the strengthening/weakening effects of the two climate systems. In the following discussion, we do not consider the data from July 2009 to June 2010 and refer to the other years (i.e., from July 2007 to June 2009 and July 2010 to June 2013) as the negative PDO–La Niña period.

Increases in primary production and POC flux in December–May for the negative PDO–La Niña period in the ETP have been suggested to be driven by strong equatorial upwelling (Kim et al., 2011; Shi & Wang, 2014). Satellite-derived NPP data for December–May increased by only 20% from 357 ± 46 mg $C{\cdot}m^{2}{\cdot}day^{-1}$ in the positive PDO period to 440 ± 48 mg $C{\cdot}m^{-2}{\cdot}day^{-1}$ in the negative PDO–La Niña

period. However, the POC flux increased threefold, suggesting higher export efficiency (i.e., *e*-ratio) during the negative PDO–La Niña period. A twofold increase in *e*-ratio accompanying the ~20% increase in NPP would result in a 2.5× increase in POC flux. Honjo et al. (1995) reported significantly higher (~1.6×) export ratios during the post-El Niño period than the El Niño period at 9°N and 140°W in the Equatorial Pacific based on sediment trap results at ~2,200 m. Murray et al. (1996) reported higher export production (i.e., double between the Equator and 13°N, except at 9°N) based on ^{234}Th measurements. Therefore, a twofold increase in the *e*-ratio appears feasible. Increases in phytoplankton cell size and mesozooplankton biomass were suggested as the potential cause of the increase in *e*-ratio (Murray et al., 1996). Flourishing of foraminifers may be a factor in the higher export, along with less remineralization due to rapid sinking. The discrepancy between NPP and POC flux might arise because the vertically generalized production model cannot adequately resolve production at the subsurface chlorophyll maximum. However, the subsurface chlorophyll maximum likely forms more strongly during higher stratification (i.e., during El Niño years; e.g., Bruland et al., 1994; Holligan et al., 1984; McLaughlin & Carmack, 2010).

4.3. Estimation of Carbon Export Based on Measured Fluxes in the Deep ETP

We investigated the importance of the biological pump in controlling the CO_2 flux between the ocean and atmosphere following the scheme of Honda et al. (1997). This was carried out in two parts. First, we estimated the export of POC and PIC (exported in the form of biogenic $CaCO_3$) out of the surface mixed layer, based on our measured fluxes and attenuation equations developed for the ETP (Berelson, 2001; Figure 4). Second, using the estimated export values for POC and PIC, we calculated the partial pressure of CO_2 (pCO_2) in the surface mixed layer in the case of no biological pump (section 4.4).

Our study site is located in the 10°N thermocline ridge area, which is the region of thermocline shoaling (<100 m) caused by divergence between the North Equatorial Countercurrent and North Equatorial Current. The satellite-derived mixed layer depth around Station KOMO for December–May deepens to a maximum of ~90 m (Kim et al., 2012). Euphotic depth (i.e., 0.1% light level) is reported to vary between 95 and 160 m in the ETP (Murray et al., 1996). We used 100 m for the reference depth of the POC and PIC exports.

Previous studies have proposed empirical equations to describe the degree of POC flux attenuation in the ETP (Berelson, 2001). POC export was estimated using the Martin equation (Martin et al., 1987). Given that we did not have data obtained simultaneously at several depths, we adopted the range of exponent "*b*" ($-0.6 < b < -0.9$) for the Martin curve reported for the ETP (Berelson, 2001):

$$\text{POC export} = \text{POC flux}_{(\text{obs})}\ (\text{d}/\text{z})^{-\text{b}} \tag{1}$$

where z, d, and $\text{flux}_{(\text{obs})}$ denote the sinking particle sampling depth (4,950 m in this study), the depth of export (100 m in this study), and observed fluxes, respectively. The *b* value ranges from −0.6 to −0.82 in the Equatorial Pacific between 5°S and 5°N, whereas it ranges from −0.73 to −0.90 at 9°N and 12°S (Berelson, 2001). The range of *b* values reflects variability in parameters such as the particle sinking speed and decomposition rate of POC. The wide range of *b* values resulted in a large uncertainty on the POC export estimates (the gray bar at a depth of 100 m in Figure 4b). For example, when the average observed POC flux (2.54 mg·m^{-2}·day^{-1}) at a water depth of 4,950 m was used, the estimated POC export ranged from 26 to 85 mg C·m^{-2}·day^{-1} (2.2 to 7.1 mmol·m^{-2}·day^{-1}; Figure 4). We used the mean value (56 mg·m^{-2}·day^{-1} or 4.6 mmol·m^{-2}·day^{-1}) and the range (±29 mg·m^{-2}·day^{-1} or 2.4 mmol·m^{-2}·day^{-1}) as the uncertainty. The *e*-ratio based on this estimate was about 0.15 ± 0.08, which is consistent with previous results obtained from the ETP (0.04–0.23) and Northeast Pacific (0.11–0.13; Buesseler et al., 2007; Henson et al., 2012; Murray et al., 1996). The T_{100} value (i.e., the ratio of POC flux at 100 m beneath the euphotic zone to POC export) based on our estimation ranges from 0.54 to 0.66. These estimates are similar to values (0.5 to 0.7) obtained for the Eastern Equatorial Pacific (Buesseler & Boyd, 2009). This suggests our estimates of the POC export are reasonable despite the large uncertainty. The *e*-ratio for December−May was about 0.25 (±0.13) in the negative PDO–La Niña period, which is more than twice that in the positive PDO period (0.10 ± 0.04).

The PIC export was estimated similarly using the empirical equation of Honda et al. (1997):

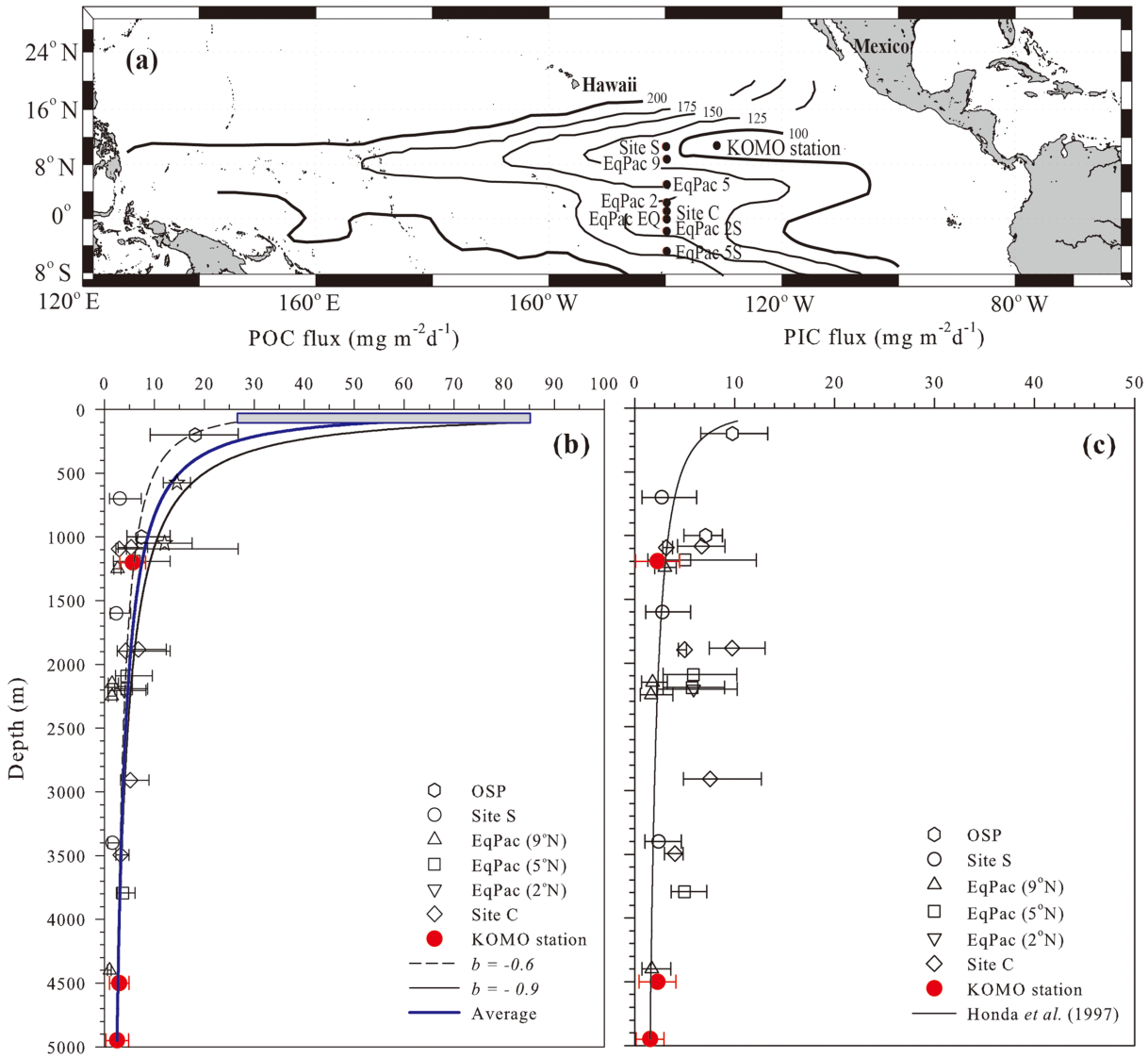

Figure 4. (a) Location of Station KOMO and other stations for which data are presented in (b) and (c). Contour lines in (a) show the thermocline depth (Wilson & Adamec, 2001). Estimated vertical attenuation of (b) particulate organic carbon (POC) flux and (c) particulate inorganic carbon (PIC) flux. POC and PIC fluxes, measured at Station KOMO and other sites in the Eastern Tropical Pacific, are also shown. The error bars are one standard deviation of the observed time-series data around the averages. The gray box at a depth of 100 m in (b) indicates the range of the estimated POC export flux. POC and PIC flux data at EqPac 9°N, 5°N, and 2°N are from Honjo et al. (1995). Data for sites S and C are from Dymond and Collier (1988). Data at Station KOMO were obtained at a depth of 1,200 m from September 2009 to April 2010 and at 4,500 m from August 2008 to February 2013 (see Data Set S1).

$$\text{PIC export} = \text{PIC flux}_{(\text{obs})}\,(d/z)^{-0.485} \tag{2}$$

Given that the attenuation of PIC flux using sediment trap data is less well studied than POC, the range of the *b* value is not available. *b* value of −0.485 is based on the observed $CaCO_3$ flux during the Joint Global Ocean Flux Study North Atlantic Bloom Experiment (Martin et al., 1993). However, PIC export is only about a third that of POC, and the uncertainty in the estimation of PIC export contributes little to the overall uncertainty in evaluation of the role of the biological pump in CO_2 outgassing. The PIC export for December–May was estimated to be 21 ± 10.1 mg·m^{-2}·day^{-1} (1.7 ± 0.8 mmol·m^{-2}·day^{-1}) in the negative PDO–La Niña period, which is also slightly more than twice that of the positive PDO period (8.3 ± 3.9 mg·m^{-2}·day^{-1} or 0.7 ± 0.3 mmol·m^{-2}·day^{-1}).

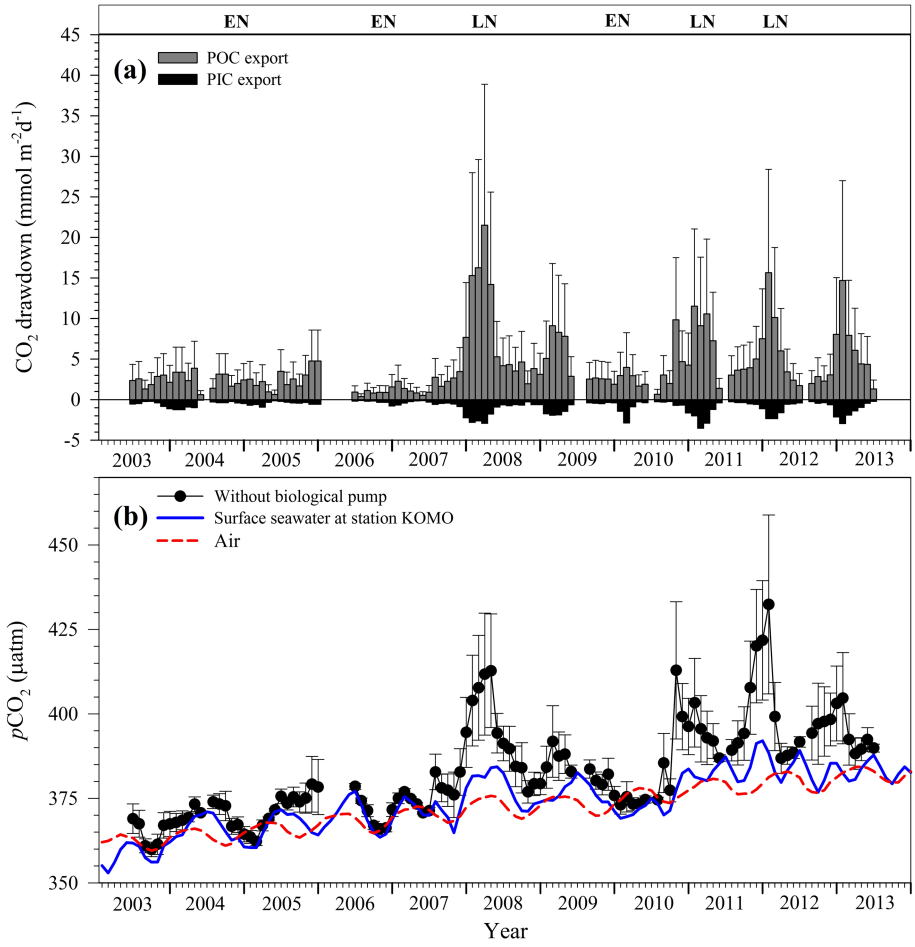

Figure 5. Effects of the biological pump and carbonate counter pump on pCO_2 in Eastern Tropical Pacific surface waters. (a) The effect of particulate organic carbon (POC) export as a CO_2 drawdown and $CaCO_3$ export as a CO_2 source in the mixed layer on CO_2 gas exchange in mmol·m^{-2}·day^{-1}. EN and LN denote El Niño and La Niña years, respectively. Blank areas indicate no data. (b) pCO_2 in the atmosphere (red dashed line) and in surface seawater (blue solid line). The pCO_2 data are modeled results based on the Surface Ocean CO_2 Atlas Version 2 (Landschützer et al., 2016). Solid circles are pCO_2 values calculated for when there was no biological pump. Error bars are based on the uncertainty associated with estimation of the POC and PIC export fluxes (see text).

4.4. Impact of Biological Processes on Surface Ocean pCO_2 at the Study Site

Export of POC and PIC from the surface water affects surface water pCO_2 and, consequently, CO_2 exchange with the atmosphere. We therefore examined the effects of POC export as a CO_2 drawdown (the so-called "biological pump") and PIC export as a CO_2 source (the so-called "carbonate counter pump"). Precipitation of $CaCO_3$ (and removal of CO_3^{2-}) facilitates dissociation of the bicarbonate ion (HCO_3^-) to H_2CO_3 and CO_3^{2-}. Production of H_2CO_3 increases pCO_2, and hence this process is called the carbonate counter pump. To account for the carbonate counter pump as a CO_2 source, the ratio of released CO_2 to carbonate precipitation (Ψ) was first estimated (Frankignoulle et al., 1994; Salter et al., 2014) and then multiplied by the PIC export. In brief, Ψ was estimated from total alkalinity (TA) and pCO_2. Time-series data of TA were estimated using polynomial algorithms based on SSS and SST (Lee et al., 2006). Monthly pCO_2 data of 1° × 1° spatial resolution, which were based on global surface ocean maps of pCO_2 reconstructed from the Surface Ocean CO_2 Atlas Version 2, were obtained from Landschützer et al. (2016). The estimated regional values of Ψ were in the range of 0.59–0.64 (average = 0.61 ± 0.01), which is consistent with the range of other reported values for the open ocean (0.60–0.63; Frankignoulle et al., 1994; Gattuso et al., 1999; Zondervan et al., 2001). The net effect of the

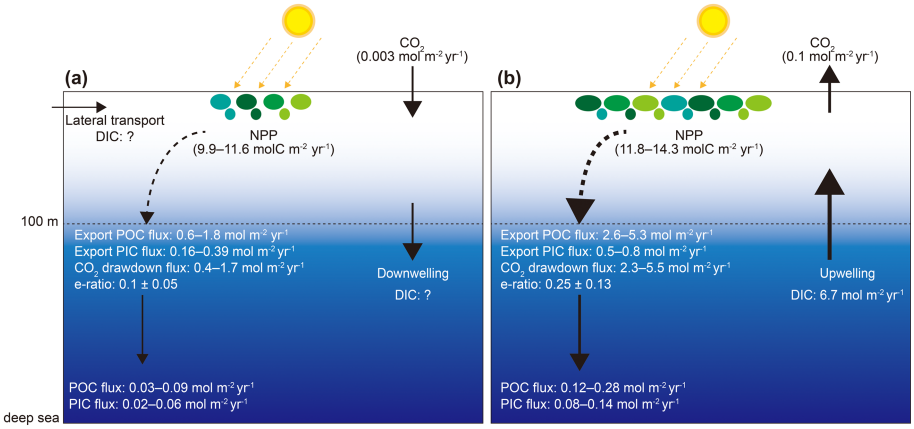

Figure 6. Schematic illustration of how a shift in the Pacific decadal oscillation from (a) a positive phase to (b) a negative phase affects the biological pump and the oceanic carbon sink in the Eastern Tropical Pacific. CO_2 gas exchange was determined based on Landschützer et al. (2016). DIC transport by upwelling was determined using the Ekman upwelling velocity (http://coastwatch.noaa.gov) and difference in DIC concentration between depths of 0 and 100 m (~310 μmol/kg). DIC = dissolved inorganic carbon; NPP = net primary production; PIC = particulate inorganic carbon; POC = particulate organic carbon.

biological pump and carbonate counter pump in the 100-m-thick surface layer was calculated as the difference between the export of POC and $\Psi \times$ PIC. The effect of the biological pump was considerably higher in the negative PDO–La Niña period than in the positive PDO period (Figure 5a). The average CO_2 drawdown by the biological pump was 8.7 ± 4.6 mmol·m^{-2}·day^{-1} for the December–May interval of the negative PDO–La Niña period and 2.4 ± 1.2 mmol·m^{-2}·day^{-1} for the December–May interval of the positive PDO period. The CO_2 source due to $CaCO_3$ production was smaller than the CO_2 drawdown by a factor of 5–8 (Figure 5a).

According to a modeling study (Landschützer et al., 2016), the present study site was a very weak CO_2 sink in 2003–2007, whereas it was a net source in 2008–2013 (Figure 5b). A study of CO_2 exchange in the Central and Eastern Equatorial Pacific also showed stronger outgassing of CO_2 during a negative PDO period (Feely et al., 2006). Upwelling of deep waters with high alkalinity and dissolved inorganic carbon (DIC) concentrations would have increased pCO_2 values much more if not suppressed by the biological pump. We further examined the potential impact of carbon export on surface ocean pCO_2 using the estimated exports of POC and PIC. One mole of PIC export is equivalent to the removal of two moles of alkalinity and one mole of DIC, while POC export is equivalent to one mole of DIC with a minor effect on alkalinity. Monthly changes in DIC and alkalinity in the 100-m-thick surface layer as a result of POC and PIC export were calculated based on this stoichiometry. Because no measurements of DIC and TA are available, the actual values for each month of the study period were determined as follows. TA values were calculated using the empirical equation as described above (Lee et al., 2006). DIC values were calculated from the estimated TA and pCO_2 data using the CO_2 SYS program (Lewis & Wallace, 1998) and the thermodynamic constants of Mehrbach et al. (1973), as refitted by Dickson and Millero (1987). The pCO_2 data are the same as described above (Landschützer et al., 2016). We then calculated the theoretical values of DIC and TA via addition of the biologically removed portions. We applied a one-month time lag between particle export and POC flux measurement at our trap depth. The results represent TA and DIC values in the case of no POC or PIC export. Finally, the theoretical pCO_2 values, for the case of no biological pump, were calculated from these TA and DIC values with the CO_2 SYS program.

The result demonstrates that the physical and chemical effects were largely suppressed by the enhanced biological pump. If it had not been suppressed by an enhanced biological pump, then the degree of supersaturation in terms of pCO_2 would have been much higher (Figure 5b). But for the biological pump, the difference in pCO_2 between the atmosphere and surface water (ΔpCO_2) would be 15.0 ± 5.5 μatm (the error is the propagated uncertainty on the estimate) instead of 3.4 ± 4.2 μatm in the negative PDO–La Niña period. Our

results imply that changes in biological processes played a major role in compensating for physical and chemical effects in the ETP (Figure 6).

5. Conclusions

Our data show a relationship between an increase in particle flux and a PDO phase shift. However, the time-series is too short for a statistically meaningful comparison with decadal variability. The particle flux shows a good correlation with ENSO variability, as also reported by Feely et al. (2006). If the biological pump is affected mainly by ENSO, a see-saw trend in biological production is expected between the western equatorial Pacific (WEP) and ETP. POC flux obtained at a depth of 1,000 m at two sites in the WEP showed a decreasing trend from July 2007 to July 2013 (Kim et al., 2014, 2017). However, it is important to note that the influence of the ENSO on the biological pump would be larger in the ETP because the primary productivity in the ETP is much higher than in the WEP.

Our results suggest that the biological pump was considerably enhanced during the negative PDO–La Niña period. Even though the biological pump did not surpass the physical and chemical effects of the upwelling, it suppressed the release of CO_2 to the atmosphere to a significant extent at the study site. The details of feedback mechanisms involving CO_2 and climate change are poorly understood and remain a key uncertainty when making predictions of future climate sensitivity to increasing atmospheric CO_2. Thus, this study may provide quantitative guidance for carbon climate modeling efforts. Furthermore, given that the frequency of extreme ENSO events is expected to increase in the near future (Cai et al., 2015), this study emphasizes the importance of monitoring the biological pump in the Tropical Pacific to examine its role in the global carbon cycle.

Acknowledgments
AcknowledgementsThis work was supported by the Korean Government's Ministry of Oceans and Fisheries (PM61150) and by Korea Institute of Ocean Science and Technology (PE99723). Particle flux and NPP data at Station KOMO are available at the National Oceanic and Atmospheric Administration's National Centers for Environmental Information's web interface (https://data.nodc.noaa.gov/cgi-bin/iso?id=gov.noaa.nodc:0201336).

References

Amador, J. A., Alfaro, E. J., Lizano, O. G., & Magaña, V. O. (2006). Atmospheric forcing of the Eastern Tropical Pacific: A review. *Progress in Oceanography*, *69*(2-4), 101–142. https://doi.org/10.1016/j.pocean.2006.03.007

Bacon, M. P., Cochran, J. K., Hirschberg, D., Hammar, T. R., & Fleer, A. P. (1996). Export flux of carbon at the equator during the EqPac time-series cruises estimated from ^{234}Th measurements. *Deep Sea Research Part II: Topical Studies in Oceanography*, *43*(4-6), 1133–1153. https://doi.org/10.1016/0967-0645(96)00016-1

Baker, E. T., Milburn, H. B., & Tennant, D. A. (1988). Field assessment of sediment trap efficiency under varying flow condition. *Journal of Marine Research*, *46*(3), 573–592. https://doi.org/10.1357/002224088785113522

Barber, R. T., & Chavez, F. P. (1991). Regulation of primary productivity rate in the equatorial Pacific. *Limnology and Oceanography*, *36*(8), 1803–1815. https://doi.org/10.4319/lo.1991.36.8.1803

Behrenfeld, M. J., & Falkowski, P. G. (1997). Photosynthetic rates derived from satellite-based chlorophyll concentration. *Limnology and Oceanography*, *42*(1), 1–20. https://doi.org/10.4319/lo.1997.42.1.0001

Behringer, D., & Xue, Y. (2004). Evaluation of the global ocean data assimilation system at NCEP: The Pacific Ocean. In *American Meteorological Society 84th Annual Meeting* (pp. 11–15).

Berelson, W. M. (2001). The flux of particulate organic carbon into the ocean interior: A comparison of four U.S. JGOFS Regional Studies. *Oceanography*, *14*(4), 59–67. https://doi.org/10.5670/oceanog.2001.07, https://doi.org/10.5670/oceanog.2001.07

Bruland, K. W., Orians, K. J., & Cowen, J. P. (1994). Reactive trace metals in the stratified central North Pacific. *Geochimica et Cosmochimica Acta*, *58*(15), 3171–3182. https://doi.org/10.1016/0016-7037(94)90044-2

Buesseler, K. O., Andrews, J. A., Hartman, M. C., Belastock, R., & Chai, F. (1995). Regional estimates of the export flux of particulate organic carbon derived from thorium-234 during the JGOFS EqPac program. *Deep Sea Research Part II: Topical Studies in Oceanography*, *42*(2-3), 777–804. https://doi.org/10.1016/0967-0645(95)00043-P

Buesseler, K. O., & Boyd, P. W. (2009). Shedding light on processes that control particle export and flux attenuation in the twilight zone of the open ocean. *Limnology and Oceanography*, *54*(4), 1210–1232. https://doi.org/10.4319/lo.2009.54.4.1210

Buesseler, K. O., Lamborg, C. H., Boyd, P. W., Lam, P. J., Trull, T. W., Bidigare, R. R., et al. (2007). Revisiting Carbon Flux Through the Ocean's Twilight Zone. *Science*, *316*(5824), 567–570. https://doi.org/10.1126/science.1137959

Cai, W., Wang, G., Santoso, A., McPhaden, M. J., Wu, L., Jin, F.-F., et al. (2015). Increased frequency of extreme La Nina events under greenhouse warming. *Nature Climate Change*, *5*(2), 132–137. https://doi.org/10.1038/nclimate2492

DeMaster, D. J. (1981). The supply and accumulation of silica in the marine environment. *Geochimica et Cosmochimica Acta*, *45*(10), 1715–1732. https://doi.org/10.1016/0016-7037(81)90006-5

Dickson, A. G., & Millero, F. J. (1987). A comparison of the equilibrium constants for the dissociation of carbonic acid in seawater media. *Deep Sea Research Part A. Oceanographic Research Papers*, *34*(10), 1733–1743. https://doi.org/10.1016/0198-0149(87)90021-5

Dymond, J., & Collier, R. (1988). Biogenic particle fluxes in the equatorial Pacific: Evidence for both high and low productivity during the 1982-1983 El Niño. *Global Biogeochemical Cycles*, *2*(2), 129–137. https://doi.org/10.1029/GB002i002p00129

Feely, R. A., Takahashi, T., Wanninkhof, R., McPhaden, M. J., Cosca, C. E., Sutherland, S. C., & Carr, M. E. (2006). Decadal variability of the air-sea CO_2 fluxes in the equatorial Pacific Ocean. *Journal of Geophysical Research*, *111*(C8), C08S90. https://doi.org/10.1029/2005JC003129

Folland, C. K., Renwick, J. A., Salinger, M. J., & Mullan, A. B. (2002). Relative influences of the Interdecadal Pacific Oscillation and ENSO on the South Pacific Convergence Zone. *Geophysical Research Letters*, *29*(13), 1643. https://doi.org/10.1029/2001GL014201

Frankignoulle, M., Canon, C., & Gattuso, J.-P. (1994). Marine calcification as a source of carbon dioxide: Positive feedback of increasing atmospheric CO_2. *Limnology and Oceanography*, *39*(2), 458–462. https://doi.org/10.4319/lo.1994.39.2.0458

Gattuso, J.-P., Allemand, D., & Frankignoulle, M. (1999). Photosynthesis and calcification at cellular, organismal and community levels in coral reefs: A review on interactions and control by carbonate chemistry. *American Zoologist*, *39*(1), 160–183. https://doi.org/10.1093/icb/39.1.160

Henson, S. A., Sanders, R., & Madsen, E. (2012). Global patterns in efficiency of particulate organic carbon export and transfer to the deep ocean. *Global Biogeochemical Cycles*, *26*(1)., GB1028 https://doi.org/10.1029/2011GB004099

Holligan, P. M., Balch, W. M., & Yentsch, C. M. (1984). The significance of subsurface chlorophyll, nitrite and ammonium maxima in relation to nitrogen for phytoplankton growth in stratified waters of the Gulf of Maine. *Journal of Marine Research*, *42*(4), 1051–1073. https://doi.org/10.1357/002224084788520747

Honda, M. C., Kusakabe, M., Nakabayashi, S., Manganini, S. J., & Honjo, S. (1997). Change in pCO_2 through biological activity in the marginal seas of the western north Pacific: The efficiency of the biological pump estimated by a sediment trap experiment. *Journal of Oceanography*, *53*, 645–662.

Honjo, S., Dymond, J., Collier, R., & Manganini, S. J. (1995). Export production of particles to the interior of the equatorial Pacific Ocean during the 1992 EqPac experiment. *Deep Sea Research Part II: Topical Studies in Oceanography*, *42*(2-3), 831–870. https://doi.org/10.1016/0967-0645(95)00034-N

Kessler, W. S. (2006). The circulation of the eastern tropical Pacific: A review. *Progress in Oceanography*, *69*(2-4), 181–217. https://doi.org/10.1016/j.pocean.2006.03.009

Kessler, W. S., McPhaden, M. J., & Weickmann, K. M. (1995). Forcing of intraseasonal Kelvin waves in the equatorial Pacific. *Journal of Geophysical Research*, *100*(C6), 10,613–10,631. https://doi.org/10.1029/95JC00382

Kim, D., Jeong, J.-H., Kim, T.-W., Noh, J. H., Kim, H. J., Choi, D. H., et al. (2017). The reduction in the biomass of cyanobacterial N_2 fixer and the biological pump in the Northwestern Pacific Ocean. *Scientific Reports*, *7*(1), 41810. https://doi.org/10.1038/srep41810

Kim, H. J., Hyeong, K., Park, J.-Y., Jeong, J.-H., Jeon, D., Kim, E., & Kim, D. (2014). Influence of Asian monsoon and ENSO events on particle fluxes in the western subtropical Pacific. *Deep Sea Research Part I: Oceanographic Research Papers*, *90*, 139–151. https://doi.org/10.1016/j.dsr.2014.05.002

Kim, H. J., Hyeong, K., Yoo, C. M., Khim, B. K., Kim, K. H., Son, J. W., et al. (2012). Impact of strong El Niño events (1997/98 and 2009/10) on sinking particle fluxes in the 10°N thermocline ridge area of the northeastern equatorial Pacific. *Deep-Sea Research Part I-Oceanographic Research Papers*, *67*, 111–120. https://doi.org/10.1016/j.dsr.2012.05.008

Kim, H. J., Kim, D., Hyeong, K., Hwang, J., Yoo, C. M., Ham, D. J., & Seo, I. (2015). Evaluation of resuspended sediments to sinking particles by benthic disturbance in the Clarion-Clipperton nodule fields. *Marine Georesources & Geotechnology*, *33*(2), 160–166. https://doi.org/10.1080/1064119X.2013.815675

Kim, H. J., Kim, D., Yoo, C. M., Chi, S. B., Khim, B. K., Shin, H. R., & Hyeong, K. (2011). Influence of ENSO variability on sinking-particle fluxes in the northeastern equatorial Pacific. *Deep-Sea Research Part I-Oceanographic Research Papers*, *58*(8), 865–874. https://doi.org/10.1016/j.dsr.2011.06.007

Lam, P. J., Coney, S. C., & Bishop, J. K. B. (2011). The dynamic ocean biological pump: Insights from a global compilation of particulate organic carbon, $CaCO_3$, and opal concentration profiles from the mesopelagic. *Global Biogeochem Cycles*, *25*, GB3009. https://doi.org/10.1029/2010GB003868

Landschützer, P., Gruber, N., & Bakker, D. C. E. (2016). Decadal variations and trends of the global ocean carbon sink. *Global Biogeochemical Cycles*, *30*, 1396–1417. https://doi.org/10.1002/2015GB005359

Lee, K., Tong, L. T., Millero, F. J., Sabine, C. L., Dickson, A. G., Goyet, C., et al. (2006). Global relationships of total alkalinity with salinity and temperature in surface waters of the world's oceans. *Geophysical Research Letters*, *33*(19), L19605. https://doi.org/10.1029/2006GL027207

Lewis, E., & Wallace, D. W. R. (1998). *Program developed for CO_2 system calculations ORNL/CDIAC-105*. Oak Ridge, Tennessee: Carbon Dioxide Information Analysis Center, Oak Ridge National Laboratory, U.S. Department of Energy.

Litzow, M. A., & Mueter, F. J. (2014). Assessing the ecological importance of climate regime shifts: An approach from the North Pacific Ocean. *Progress in Oceanography*, *120*, 110–119. https://doi.org/10.1016/j.pocean.2013.08.003

Loubere, P. (2000). Marine control of biological production in the eastern equatorial Pacific Ocean. *Nature*, *406*(6795), 497–500. https://doi.org/10.1038/35020041

Mantua, N. J., & Hare, S. R. (2002). The Pacific decadal oscillation. *Journal of Oceanography*, *58*(1), 35–44. https://doi.org/10.1023/A:1015820616384

Martin, J. H., Fitzwater, S. E., Gordon, R. M., Hunter, C. N., & Tanner, S. J. (1993). Iron, primary production and carbon-nitrogen flux studies during the JGOFS North Atlantic Bloom Experiment. *Deep Sea Research Part II: Topical Studies in Oceanography*, *40*(1-2), 115–134. https://doi.org/10.1016/0967-0645(93)90009-C

Martin, J. H., Knauer, G. A., Karl, D. M., & Broenkow, W. W. (1987). VERTEX: Carbon cycling in the northeast Pacific. *Deep Sea Research Part A. Oceanographic Research Papers*, *34*(2), 267–285. https://doi.org/10.1016/0198-0149(87)90086-0

McLaughlin, F. A., & Carmack, E. C. (2010). Deepening of the nutricline and chlorophyll maximum in the Canada Basin interior, 2003-2009. *Geophysical Research Letters*, *37*(24), L24602. https://doi.org/10.1029/2010GL045459

Mehrbach, C., Culberson, C. H., Hawley, J. E., & Pytkowicx, R. M. (1973). Measurement of the apparent dissociation constants of carbonic acid in seawater at atmospheric pressure. *Limnology and Oceanography*, *18*(6), 897–907. https://doi.org/10.4319/lo.1973.18.6.0897

Murray, J. W., Young, J., Newton, J., Dunne, J., Chapin, T., Paul, B., & McCarthy, J. J. (1996). Export flux of particulate organic carbon from the central equatorial Pacific determined using a combined drifting trap-234Th approach. *Deep Sea Research Part II: Topical Studies in Oceanography*, *43*(4-6), 1095–1132. https://doi.org/10.1016/0967-0645(96)00036-7

Newman, M., Alexander, M. A., Ault, T. R., Cobb, K. M., Deser, C., di Lorenzo, E., et al. (2016). The Pacific decadal oscillation, revisited. *Journal of Climate*, *29*(12), 4399–4427. https://doi.org/10.1175/JCLI-D-15-0508.1

Newman, M., Compo, G. P., & Alexander, M. A. (2003). ENSO-Forced variability of the Pacific decadal oscillation. *Journal of Climate*, *16*(23), 3853–3857. https://doi.org/10.1175/1520-0442(2003)016<3853:EVOTPD>2.0.CO;2

Pennington, J. T., Mahoney, K. L., Kuwahara, V. S., Kolber, D. D., Calienes, R., & Chavez, F. P. (2006). Primary production in the eastern tropical Pacific: A review. *Progress in Oceanography*, *69*(2-4), 285–317. https://doi.org/10.1016/j.pocean.2006.03.012

Peterson, W. T., & Schwing, F. B. (2003). A new climate regime in northeast pacific ecosystems. *Geophysical Research Letters*, *30*(17), 1896. https://doi.org/10.1029/2003GL017528

Reynolds, R. W., Smith, T. M., Liu, C., Chelton, D. B., Casey, K. S., & Schlax, M. G. (2007). Daily high-resolution-blended analyses for sea surface temperature. *Journal of Climate*, *20*(22), 5473–5496. https://doi.org/10.1175/2007jcli1824.1

Salter, I., Schiebel, R., Ziveri, P., Movellan, A., Lampitt, R., & Wolff, G. A. (2014). Carbonate counter pump stimulated by natural iron fertilization in the Polar Frontal Zone. *Nature Geoscience*, *7*(12), 885–889. https://doi.org/10.1038/ngeo2285

Shi, W., & Wang, M. (2014). Satellite-observed biological variability in the equatorial Pacific during the 2009–2011 ENSO cycle. *Advances in Space Research*, *54*(9), 1913–1923. https://doi.org/10.1016/j.asr.2014.07.003

Strutton, P. G., & Chavez, F. P. (2000). Primary productivity in the equatorial Pacific during the 1997–1998 El Niño. *Journal of Geophysical Research*, *105*(C11), 26,089–26,101. https://doi.org/10.1029/1999JC000056

Takahashi, T., Sutherland, S. C., Feely, R. A., & Cosca, C. E. (2003). Decadal variation of the surface water PCO_2 in the western and central Equatorial Pacific. *Science*, *302*(5646), 852–856. https://doi.org/10.1126/science.1088570

Takahashi, T., Sutherland, S. C., Wanninkhof, R., Sweeney, C., Feely, R. A., Chipman, D. W., et al. (2009). Climatological mean and decadal change in surface ocean pCO_2, and net sea-air CO_2 flux over the global oceans. *Deep Sea Research Part II: Topical Studies in Oceanography*, *56*(8-10), 554–577. https://doi.org/10.1016/j.dsr2.2008.12.009

Tollefson, J. (2014). Climate change: The case of the missing heat. *Nature*, *505*(7483), 276–278. https://doi.org/10.1038/505276a

Verardo, D. J., Froelich, P. N., & McIntyre, A. (1990). Determination of organic carbon and nitrogen in marine sediments using the Carlo Erba NA-1500 Analyzer. *Deep Sea Research*, *37*(1), 157–165. https://doi.org/10.1016/0198-0149(90)90034-S

Wang, S., Huang, J., He, Y., & Guan, Y. (2014). Combined effects of the Pacific decadal oscillation and El Niño-Southern Oscillation on global land dry–wet changes. *Scientific Reports*, *4*(4), 6651. https://doi.org/10.1038/srep06651

Wefer, G., & Fischer, G. (1993). Seasonal patterns of vertical particle flux in equatorial and coastal upwelling areas of the eastern Atlantic. *Deep Sea Research Part I: Oceanographic Research Papers*, *40*(8), 1613–1645. https://doi.org/10.1016/0967-0637(93)90019-Y

Wilson, C., & Adamec, D. (2001). Correlations between surface chlorophyll and sea surface height in the tropical Pacific during the 1997-1999 El Niño-southern oscillation event. *Journal of Geophysical Research*, *106*(C12), 31,175–31,188. https://doi.org/10.1029/2000JC000724

Wu, C.-R. (2013). Interannual modulation of the Pacific decadal oscillation (PDO) on the low-latitude western North Pacific. *Progress in Oceanography*, *110*, 49–58. https://doi.org/10.1016/j.pocean.2012.12.001

Zondervan, I., Zeebe, R. E., Rost, B., & Riebesell, U. (2001). Decreasing marine biogenic calcification: A negative feedback on rising atmospheric pCO_2. *Global Biogeochemical Cycles*, *15*(2), 507–516. https://doi.org/10.1029/2000GB001321